Specific heat measurements of the lattice contribution and spin-density-wave transition in $(TMTSF)_2X$ (X = PF_6 and AsF_6) and $(TMTTF)_2Br$ salts

1999 J. Phys.: Condens. Matter 11 5083

(http://iopscience.iop.org/0953-8984/11/26/310)

J. Phys.: Condens. Matter **11** (1999) 5083–5098. Printed in the UK PII: S0953-8984(99)01162-5

Specific heat measurements of the lattice contribution and spin-density-wave transition in $(TMTSF)_2X$ (X = PF_6 and AsF_6) and $(TMTTF)_2Br$ salts

Hongshun Yang†‡, J C Lasjaunias† and P Monceau†

† Centre de Recherches sur les Très Basses Températures, laboratoire associé à l'Université Joseph Fourier, CNRS, BP 166, 38042 Grenoble Cédex 9, France

‡ Physics Department, University of Science and Technology of China, Hefei, Anhui 230026, People's Republic of China

Received 22 January 1999, in final form 13 April 1999

Abstract. The specific heats of the quasi-one-dimensional organic compounds $(TMTSF)_2X$ (X = PF_6, AsF_6 and ClO_4) and $(TMTTF)_2Br$ were measured over the temperature range from 1.8 to 40 K. The lattice contribution follows a T^3-law only in a small temperature range below 3 K, and shows a typical bump in C/T^3 at about 7.0 K for every compound (4 K for $(TMTSF)_2ClO_4$). We interpret this behaviour as a phonon dimensionality crossover from a low-T tridimensional behaviour, towards a lower-dimensionality T^α-behaviour (with $\alpha = 2.3$ to 2.5) above 3 K, plus two additional Einstein modes in agreement with the frequencies of soft lattice modes detected by far-infrared spectroscopy. The spin-density-wave (SDW) transition temperature was found to take the values 12.2, 12.4 and 11.7 K for the compounds $(TMTSF)_2PF_6$, $(TMTSF)_2AsF_6$ and $(TMTTF)_2Br$, respectively. The magnitude of the SDW transition anomaly is 4.5%, 2.5% and less than 1% of the total specific heat for each sample, respectively. The magnitude of the specific heat anomaly for $(TMTSF)_2PF_6$ is too large to be explained by the electron spin contribution alone, which implies that the lattice is also involved in the transition. From our accurate measurements, we confirm that the SDW transition is a second-order transition without any characteristics of first order, like hysteresis and latent heat. The specific heat was found to be time dependent over the whole measurement temperature range as its value is quite sensitive to the kinetics process for all three compounds.

1. Introduction

The spin-density-wave (SDW) dynamics in the organic chainlike salts of general formula $(TMTCF)_2X$ (C = Se for tetramethyltetraselenafulvalene TMTSF or S for tetramethyltetrathiafulvalene TMTTF, and X = PF_6, AsF_6, ReO_4, ClO_4, Br etc) has attracted much interest in recent years. The selenium salts or Bechgaard salts exhibit a fascinating variety of electronic and structure behaviour, including SDWs, superconductivity, magnetic-field-induced spin-density waves (FISDWs), anion order–disorder transitions [1, 2], quantized Hall resistance reminiscent of the quantum Hall effect [3], metallic re-entrance at high fields [4] and glasslike transition at 3 K observed both by NMR and specific heat measurements [5–8]. The replacement of selenium by sulphur or the use of a different anion can be regarded as a means of 'tuning' the low-temperature properties [2].

The triclinic unit cell of these salts contains one anion and two donor molecules with a zigzag packing of flat molecules along the high-conductivity axis. It is well known that most of these compounds exhibit a SDW transition at about 12 K at ambient pressure. Calorimetric

0953-8984/99/265083+16$19.50

measurements for $(TMTSF)_2PF_6$ show that the specific heat jump at the transition deviates from the shape expected from mean-field theory [9]. The muon spin-rotation (μ^+SR) measurements show that the temperature dependence of the order parameter is very similar to that for 2D Heisenberg systems [10]. NMR line-shape analyses for $(TMTSF)_2PF_6$ indicate that the wave vectors of the SDW states studied so far are incommensurate with the underlying lattice [11,12] but close to (1/2, 1/4, 0). In the case of the compound $(TMTTF)_2Br$, the spin modulation is commensurate with a wave vector (1/2, 1/4, 0) [13, 14].

Specific heat measurements allow us to detect structural, electronic and magnetic transitions, and to determine the electron and phonon contributions. This can give very important information about the electron density of states at the Fermi level $N(E_F)$, the electron–phonon coupling and the magnetic fluctuations. In this paper, we report on new specific heat results for $(TMTSF)_2PF_6$, $(TMTSF)_2AsF_6$, $(TMTSF)_2ClO_4$ and $(TMTTF)_2Br$ single crystals. The main purposes of this calorimetric study were: (1) to check whether there is a similarity of the thermodynamical properties of these quasi-1D organic structures as has been found in the cases of 1D charge-density-wave (CDW) compounds such as blue bronze, $(TaSe_4)_2I$, and platinum chains (KCP) [15]; (2) to carefully investigate the anomalies related to the SDW transition.

Concerning the first point, we found that for the four salts investigated the phonon contribution presents a Debye behaviour ($C \sim T^3$) only below 3 K. Above this temperature the specific heat can be described by the law $C \sim T^\alpha$ with $\alpha = 2.4 \pm 0.1$, plus the contribution of two additional low-energy Einstein modes. We confirm that the SDW transition is of second-order type. In the case of $(TMTSF)_2PF_6$ the specific heat anomaly at the SDW phase transition cannot be explained by the electron contribution alone, but implies a lattice contribution which may originate from the $2k_F$ mixed CDW–SDW modulation, as recently revealed by x-ray measurements [16]. Over the whole T-range investigated, the specific heat is time dependent for these three compounds, as a result of its sensitivity to the experimental kinetics conditions.

2. Experimental details

Single crystals (needles) of $(TMTSF)_2PF_6$, $(TMTSF)_2AsF_6$, $(TMTSF)_2ClO_4$ and $(TMTTF)_2Br$ (for short: PF_6, AsF_6, ClO_4 and Br) were synthesized by standard electro-chemical methods [17, 18]. The typical size of the needles is about $0.5 \times 0.5 \times 3$ mm^3. A sample consists of hundreds of tiny needle crystals. The sample weights for PF_6, AsF_6, Br and ClO_4 were 180, 91, 68 and 184 mg, respectively. For these samples, 6.0, 7.5, 13.0 and 12.6 mg of the grease Apiezon *N* were used respectively to improve the thermal contact between the small single crystals and the silicon sample holder, in a method previously described in reference [6]. For $(TMTSF)_2PF_6$, we have made measurements on samples from the same batch as for previous specific heat measurements [7, 8].

The specific heat measurement was performed with a transient-heat-pulse technique using a similar arrangement to that in our previous investigations [6–8, 19]. The specific heat C_p is calculated from the increment of the temperature $\Delta T = T - T_0$ that occurs during a heat pulse (duration: 0.2 s at 1.7 K to several tens of seconds at 40 K—always 1/20 of the relaxation time τ) by using the exponential decay of the temperature increase $T(t) - T_0 = (T_p - T_0)\exp(-t/\tau)$, with the relaxation time $\tau = C_p R_\ell$, where C_p is the total heat capacity and R_ℓ the thermal resistivity of the thermal link to the regulated cold sink. In the experiments, $\Delta T/T_0$ is always kept between 1% and 3%, T_0 being the reference temperature before the heating pulse, which can be stabilized within 5×10^{-4} over several hours. Experiments were performed in two cryostats: a ^{4}He-pumped cryostat, between 1.8 and 40 K, or a dilution ^{3}He/^{4}He refrigerator, between 0.1 and 7 K, with different thermal links R_ℓ (larger in the case of the dilution refrigerator). By convention, we will use the terms 'short' transient heat pulses for the data

obtained in the ^{4}He cryostat with shorter τ and 'long' transient heat pulses for the data obtained in the dilution refrigerator with longer τ. For instance, at 4 K for the AsF_6 sample, $\tau = 4$ s for the short transient heat pulses, and $\tau = 13$ s for the long ones.

The physical properties of the Bechgaard salts can be sensitive to the cooling rate. This is particularly the case for $(TMTSF)_2ClO_4$, due to an ordering transition of the non-centrosymmetric ClO_4^- anions which occurs at $T = 24$ K. A complete ordering takes place only if the temperature is swept very slowly in the transition range and the ground state is then superconducting [1]. In contrast, if the sample is quenched from above the anion ordering transition temperature, this ordering cannot occur. In this case $(TMTSF)_2ClO_4$ undergoes a SDW transition at around 3–5 K depending on the quenching rate. Despite the fact that no such ordering transition is expected to occur for the other three compounds characterized by the centrosymmetric anions PF_6^-, AsF_6^- and Br^-, great care was taken to detect any possible effect of the change of the cooling rate for the PF_6, AsF_6 and Br samples. In the present experiment (with the ^{4}He cryostat) these three samples were cooled in vacuum naturally from room temperature, to liquid nitrogen temperature which usually takes about 15 hours. Further (slow) cooling from 77 K down to 4.2 K usually takes 10 hours with a cooling rate at the SDW transition at 12 K of about 0.3 K h^{-1}, whereas fast cooling corresponds to a rate of about 10 K min^{-1} at 12 K. No difference between the specific heat data for the fast and the slow cooling from 77 K down to 1.8 K for these three samples was detected within the experimental uncertainty.

The results concerning the ClO_4 sample given in this paper were obtained by quenching the temperature from 40 K to 20 K (through the anion ordering temperature) at a rate of 3.3 K s^{-1}, which yields the SDW transition at 4.5 K. The effect of the cooling rate for the ClO_4 system will be published separately [20]. The specific heat of the sample holder has been measured in other separate experiments and its contribution to the total heat capacity was about 40–50%. The data for the specific heat of the grease Apiezon *N* were taken from reference [21].

3. Experimental results and discussion

3.1. Phonon dimensionality crossover and low-frequency modes

The specific heat C_p of PF_6 (the data are taken from reference [7]), together with our new data for AsF_6, Br and ClO_4 (the quenched-SDW state) are presented in figure 1 in the form of the temperature dependences of C_p/T^3 from 1.8 to 40 K. The SDW transition appears as a shallow anomaly in the total specific heat at $T_c = 12.2$, 12.4, 11.7 and 4.5 K for the four compounds, respectively. The anion ordering for quenched ClO_4 is also clearly detectable from the anomaly at 24 K. In the case of PF_6, we have previously pointed out that the abrupt jump at $T = 3.5$ K was observed under particular timescale conditions (by the transient-heat-pulse technique), whereas it disappears under quasi-adiabatic conditions (see the difference below 5 K between the two series of data obtained by a quasi-adiabatic technique (▲) and by a transient-heat-pulse technique (□)) [7]. We have ascribed this jump as resulting from a glasslike transition due to the freezing in of internal degrees of freedom of the disordered SDW [22]. Our previous low-temperature data indicate that the lattice contribution (obtained after subtracting the contribution of low-energy excitations) C_p/T^3 versus T is rather flat below 3.0 K down to 0.5 K for PF_6 [6], AsF_6 [23] and Br [24], so the Debye law $C_p = \beta T^3$ is quite good for describing the lattice specific heat in the low-T limit, with $\beta = 14.5 \pm 0.5$ mJ mol^{-1} K^{-4} for PF_6 [6], 13 mJ mol^{-1} K^{-4} for AsF_6 [23] and 7.8 mJ mol^{-1} K^{-4} for Br [24]. The βT^3-limit is also observed for the present series of data for T below 3 K in the case of AsF_6 and ClO_4. The βT^3-limits obtained for PF_6 from previous measurements [6] and for AsF_6, ClO_4 and Br

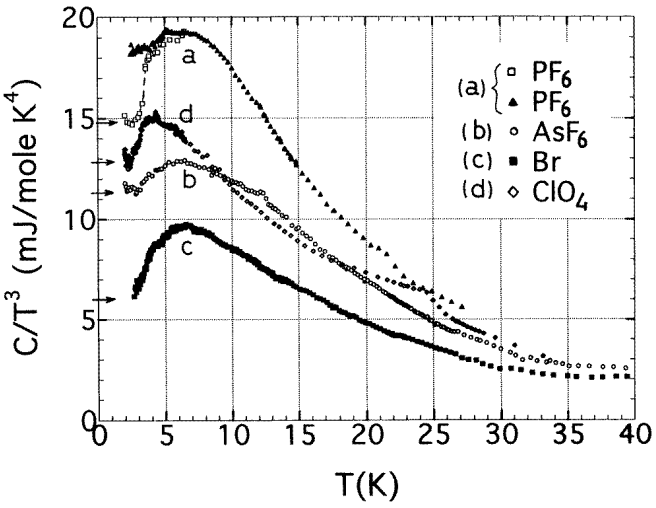

Figure 1. Comparison of the temperature dependences of C_p/T^3 for $(TMTSF)_2PF_6$ (from reference [7]; the effect of the experimental timescale below 5 K (□ and ▲ data) is discussed in this reference), $(TMTSF)_2AsF_6$, $(TMTTF)_2Br$ and $(TMTSF)_2ClO_4$ (the quenched-SDW state: this work and reference [20]). The arrows indicate the low-temperature cubic-regime βT^3 observed below 3 K (numerical values are reported in table 1 with the corresponding Debye temperatures).

Table 1. Parameters used in fitting the lattice contribution for the three compounds ($(TMTSF)_2PF_6$, $(TMTSF)_2AsF_6$ and $(TMTTF)_2Br$) with the formulae $C_p = \beta T^3 + bC_{\Theta_1} + cC_{\Theta_2}$ ($T < 2.5\,\mathrm{K} = T^*$) and $C_p = aT^\alpha + bC_{\Theta_1} + cC_{\Theta_2}$ ($T > 2.5$ K). All parameters are in units of mJ mol^{-1} K^{-1} for C_p. θ_D is the Debye temperature extracted from the lattice β-coefficient. For $(TMTSF)_2ClO_4$ (the quenched-SDW state: this work), only β and θ_D are reported; values for the metallic state from reference [39] are also reported for comparison.

System	α	a	Θ_1 (K)	b	Θ_2 (K)	c	β (mJ mol^{-1} K^{-4})	θ_D (K)
PF_6	2.4	28	35	0.77	65	1.74	14.8	198
AsF_6	2.3	20	30	0.33	65	2.5	11.3	217
Br	2.5	8.0	30	0.30	65	1.5	6.0	260
			ClO_4 (SDW state: this work)				12.8	205
			ClO_4 (metallic state: from reference [39])				11.4	213

from the present experiments are shown by the arrows in figure 1. The corresponding Debye temperatures, θ_D, extracted from β using the usual formula, $\beta = \frac{12}{5} r R(\pi^4/\theta_D^3)$, with R the gas constant and r the number of atoms per formula unit [25], are reported in table 1.

From figure 1, one can see that C_p/T^3 presents a bump with a maximum located at about 7.0 K for PF_6, AsF_6 and Br. For the ClO_4 (quenched-SDW state) sample, the bump is located at a lower temperature (about 4.0 K). Such an upward deviation of the specific heat from the usual Debye T^3-law is currently ascribed to low-energy phonon modes. Thus, it has been previously shown that low-frequency modes, described as Einstein oscillators, contribute to the specific heat of other quasi-1D compounds, as a maximum in C_p/T^3 at 12 K for blue bronze $K_{0.3}MoO_3$ [26, 27], 7 K for the Pt-chain compound 'KCP' [28] and even 1.7 K for $(TaSe_4)_2I$ [29]. They originate from low-lying transverse acoustic or optical modes, related to the 1D structural property [15]. An alternative explanation lies in phason excitations, originating from the incommensurate charge-density waves of these compounds, and modelled by a Debye-like spectrum using two cut-off frequencies [29]. In the case of

organic compounds, the low-energy 'intra'-molecular phonon modes have been revealed by far-infrared spectroscopy [30, 31].

Since the general tendencies of C_p/T^3 versus temperature are the same for PF_6, AsF_6 and Br, we have plotted normalized C_p/T^3 versus temperature for PF_6 (unmodified), AsF_6 ($1.5 \times C_p/T^3$) and Br ($2 \times C_p/T^3$), as shown in figure 2. The solid curve is the fit for PF_6 as described later in the text. We see that the three series of data almost merge into a single curve over the whole measurement temperature range except for the lowest temperature below the peak. Since the positions of the peaks are the same for the three samples, we can rule out the possibility that the bumps originate from the vibrations of the anions (i.e., PF_6^-, AsF_6^- and Br^-) independently of the rest of the lattice. The large difference in molecular weight of the anions (by a factor of 2.4 for AsF_6 and Br) should result in a large difference in the vibrational frequencies of the Einstein oscillators. In this case, we should have measured different peak positions in the plots of C_p/T^3 versus temperature T.

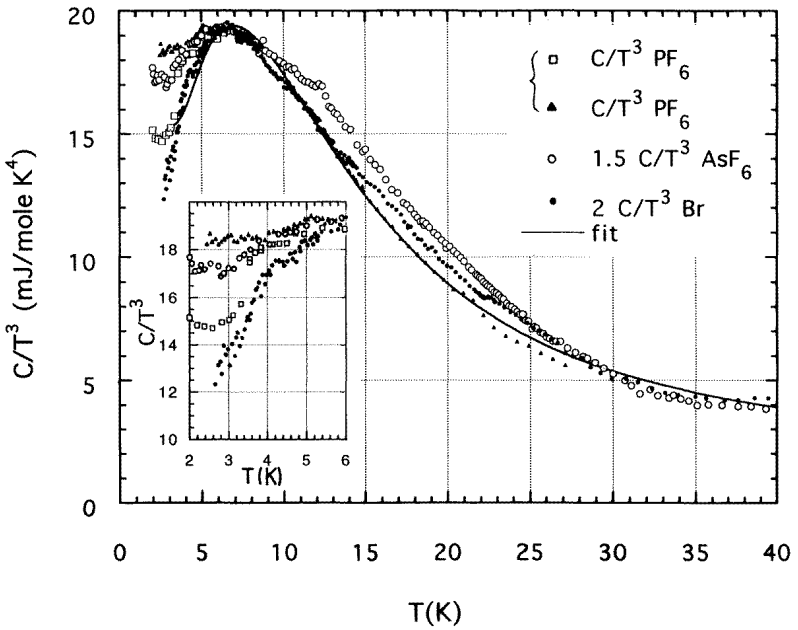

Figure 2. Normalized C_p/T^3 versus temperature for $(TMTSF)_2PF_6$ (reference value: □ and ▲ data), $(TMTSF)_2AsF_6$ ($1.5 \times C_p/T^3$: ○ data) and $(TMTTF)_2Br$ ($2 \times C_p/T^3$: ● data). The solid curve is the fit for the $(TMTSF)_2PF_6$ data as described in the text. The inset shows the T-range between 2 K and 6 K.

Independently of the contribution of the Einstein modes, the substantial decrease of C_p/T^3 in the high-T range cannot be explained by the usual assumption of deviation from the T^3-law which starts at $T = \theta_D/20$, at least. For instance, in the case of PF_6 with $\theta_D = 200$ K [6], the generalized Debye function starts to deviate from the cubic regime above 15 K, and at 25 K the deviation reaches 10%, whereas the observed deviation is larger than a factor of two. Thus we have tried to describe the variation of C/T^3 using a temperature-dependent phonon background T^α, with $\alpha < 3$. Figure 3 shows the process of fitting for PF_6, based on the assumption of two main contributions: an acoustic background which changes from a cubic regime below a crossover temperature T^* towards T^α above, plus two additional Einstein modes, the frequencies of which are based on far-IR measurements, available in the cases of

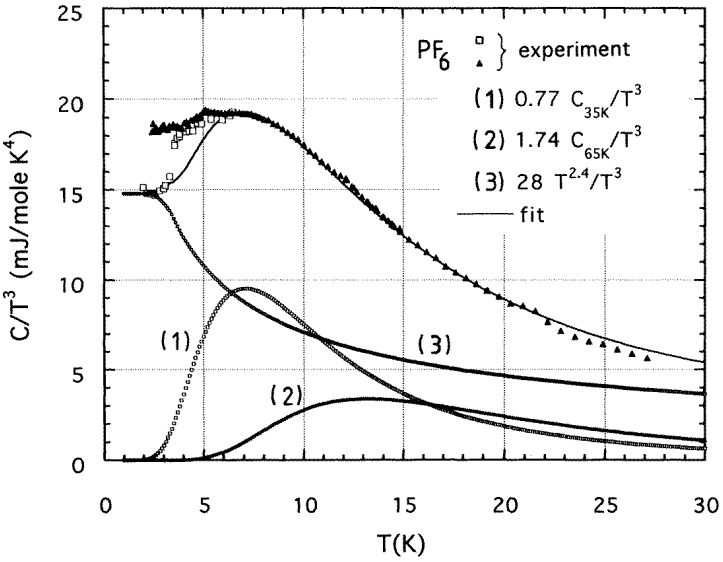

Figure 3. The process of the fitting for $(TMTSF)_2PF_6$, for the □ data below 5 K, obtained by the transient-heat-pulse technique (the ▲ show data obtained by the quasi-adiabatic technique). The specific heat is analysed following formula (1). The temperature T^* of the crossover between the T^3-regime ($T < T^*$) and the T^α-regime ($\alpha = 2.4$) ($T > T^*$) is 2.5 K.

PF_6 [30] and ClO_4 [31] salts. The following expression was used to fit the data:

$$C_p = \begin{cases} \beta T^3 + bC_{\Theta_1} + cC_{\Theta_2} & (T < T^*) \\ aT^\alpha + bC_{\Theta_1} + cC_{\Theta_2} & (T > T^*). \end{cases} \tag{1}$$

In the formula, C_Θ is the Einstein specific heat for N (Avogadro number) independent vibrational modes. Thus, $C_\Theta = 3R(\Theta/T)^2 \exp(\Theta/T)/[\exp(\Theta/T) - 1]^2$, where R is the gas constant, Θ the Einstein temperature.

Note that β is not a free parameter: it is determined from the lower-T limit of C/T^3 (see the arrows in figure 1). In the case of PF_6, this value is well established from our previous analysis of data obtained between 0.5 and 3 K [6]. The Einstein frequencies are closely related to the far-IR reflectivity measurements. In the case of PF_6 [30], for the electric field applied parallel to the $\vec{a}$-axis, two sharp peaks were measured at 18 cm^{-1} and 45 ± 5 cm^{-1} (equivalent to 26 K and 64 ± 7 K). Two similar modes, but shifted in frequency, were observed for metallic ClO_4 salt at 7 and 25 or 29 cm^{-1} in reference [31]. Their phonon origin was established in reference [31b].

A possible fitting is shown for PF_6 in figure 3 with parameters $\beta = 14.8$ mJ mol^{-1} K^{-4}, $T^* = 2.5$ K, $\alpha = 2.4$, $a = 28$ mJ mol^{-1} $K^{-3.4}$, $b = 0.77$, $c = 1.74$ (if C_p is expressed in mJ mol^{-1} K^{-1}), $\Theta_1 = 35$ K and $\Theta_2 = 65$ K. Similar fittings are obtained for AsF_6 and Br with the parameters reported in table 1. For PF_6, the Θ_1-value is chosen to be slightly larger than the IR frequency (26 K), to better take into account the broad maximum centred at 7 K. For the AsF_6 and Br compounds, a common value $\Theta_1 = 30$ K was obtained. For the three compounds PF_6, AsF_6 and Br, the second Einstein temperature $\Theta_2 = 65$ K is in exact coincidence with that of the far-IR vibrational mode measured for PF_6. The shift of the maximum of C/T^3 from 7 K for PF_6 to 4 K for ClO_4 (figure 1) is also in agreement with the related shift to 7 and 25 cm^{-1} of the two first IR modes. These properties strongly support the present analysis. The

similarity of the Θ_1- and Θ_2-values for the three compounds (PF_6, AsF_6 and Br) is evident from the unicity shown by the reduced diagram of figure 2.

Similar crossover temperatures of $T^* = 2.5$ K are also obtained, but slightly different α-values (from 2.3 for AsF_6 to 2.5 for Br). Again, we want to stress that an analysis based on the usual Debye function for the acoustic background, plus the necessary Einstein modes, would completely fail for $T \gtrsim 10$ K. This is why the only way to proceed with the analysis is to introduce a T^α-variation ($\alpha < 3$) for the acoustic contribution above the crossover temperature T^*. The similar crossover temperatures and close values of α reflect the common vibrational properties of the molecular backbone TMTCF.

Strong deviations from the Debye behaviour, as illustrated by a value of the temperature exponent α lower than 3, are characteristic of a system with anisotropic force constants. This kind of phenomenon was observed for polymers, such as crystalline metallic polysulphur nitride $(SN)_x$ [32], hexagonal selenium [33] and crystalline polyethylene [33, 34], and also for low-dimensional CDW compounds such as $NbSe_3$ [19, 35] and the Pt-chain compound KCP [28]. For the polysulphur nitride $(SN)_x$, the lattice contribution to the specific heat deviates from Debye behaviour near 4 K, changing from a T^3- to $T^{2.7}$-dependence and then to a linear temperature dependence as the temperature increases up to 80 K. For the hexagonal selenium and crystalline polyethylene, the T^3-dependence of the specific heat persists up to above 10 K and then C_p begins to saturate. An Einstein localized mode, and consequently a bump in the plot of C_p/T^3 versus T, was also found for partially crystalline polyethylene [34]. For $NbSe_3$ [35], one can estimate the temperature T^* of the crossover between the T^3- and $T^{2.9}$-regimes to be around 1 K, whereas for KCP, a lattice $T^{2.8}$-contribution is consistent with the analysis of data over the whole temperature range investigated, from ~0.2 K to 30 K, which means that T^* lies below ~0.5 K [28].

A sub-cubic regime for the lattice contribution can be interpreted within the model of Genensky and Newell [36] as originating in the strong anisotropy of the force constants along or between adjacent chains. In an intermediate-temperature range, the abnormal contribution varying as $T^{2.5}$ for the transverse vibrations and the regular T^3-contribution from longitudinal vibrations result in a total specific heat varying as T^α, with the power-law coefficient α in the range between 2.5 and 3. At low temperatures, the temperature T^* of the crossover between the low-T Debye regime and the T^α-regime is determined by the ratio $\Gamma/\sqrt{4\kappa}$ [36], Γ being the force constant of adjacent chains and κ the force constant for bending along the chains.

Our present analysis yields a T^*-value of about 2.5 K, a temperature lower than in the case of polymeric chain compounds like Se or polyethylene, but the power-law exponent α is 2.4 ± 0.1, close to the limit case for the Genensky–Newell model, which implies that the contribution of the transverse modes is predominant in the lattice specific heat.

3.2. Time dependence of the specific heat

A characteristic phenomenon in the $(TMTCF)_2X$ compounds is a time-dependent specific heat. The trivial explanation of a poor thermal diffusivity of the samples can be ruled out. All of the transient-pulse measurements were performed with a heating time t_h much smaller than the relaxation time τ—typically $t_h/\tau \sim 1/20$; we have verified that thermal diffusive equilibrium was achieved during the heating time.

Figure 4 shows the comparison of C_p/T^3 versus temperature for PF_6 measured by ac and pulse-relaxation methods [9] at UCLA and by transient-heat-pulse and quasi-adiabatic [7, 37] methods in Grenoble.

There is a large discrepancy among the sets of data measured for very different experimental conditions:

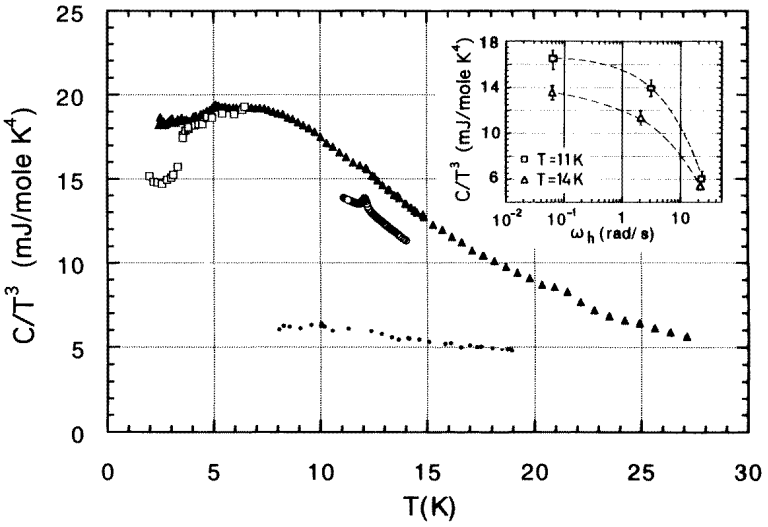

Figure 4. Comparison of C_p/T^3 versus temperature for $(TMTSF)_2PF_6$, measured with quasi-adiabatic (▲ data (reference [7])), transient-heat-pulse (□ data (reference [7]) and ○ data (this work)) and pulse-relaxation techniques (● data (reference [9])). Inset: the frequency dependence of the specific heat for $(TMTSF)_2PF_6$ at two temperatures: 11 and 14 K. The frequency ω_h is defined in terms of the heating period by $\omega_h = 2\pi/t_h$.

(a) The first difference is as regards the duration of the heating pulse. The duration of the heating, t_h, is 100 s for the adiabatic technique between 2.5 and 25 K (▲ symbols in figure 4; sample mass 408 mg), 2–3 s for the short-heat-pulse method between 11 K and 14 K (○ symbols; sample mass 180 mg), 0.5 to 1 s for the long-heat-pulse method below 6 K (□ symbols; sample mass 110 mg) and 0.29 s for the ac method between 11.5–12.6 K. As there is no indication in reference [9] of the duration of the pulses in the pulse-relaxation technique, and no difference in the data to which the ac method was applied, we report the data obtained by the pulse-relaxation method (● symbols; sample mass a few mg) between 8 and 20 K supposing them to correspond to the same excitation frequency of 3.5 Hz (or $t_h = 0.29$ s). If we define the frequency of the thermal disturbance (the heating pulse) as $\omega = 2\pi/t_h$, then we can see the frequency dependence of the specific heat for PF_6, as shown in the inset of figure 4 in a C_p/T^3 diagram. It appears that C_p/T^3 saturates at low frequency and decreases rapidly with increasing frequency either above the SDW transition temperature (at $T = 14.0$ K) or below the SDW transition temperature (at $T = 11.0$ K). From the inset in this figure, we can conclude that the effect of the frequency dependence of the specific heat becomes stronger with decreasing temperature.

(b) The second difference is as regards the relaxation times τ $(=R_\ell C_p)$ for the samples, due to the different configurations of the sample holders used in the different methods. We stress that the thermal transients after a heat pulse are always exponential over the whole temperature range investigated, contrary to the case for experiments below 1 K. Indeed, in that T-range, a different kind of time-dependent effect occurs in these systems, which appears as a progressive deviation from the exponential regime with decreasing temperature (see reference [8] for PF_6 and reference [38] for TaS_3), resulting from the long relaxation time of low-energy excitations inherent to the disordered character of the density-wave ground state.

For the adiabatic method, in the case of PF_6, the total data acquisition including the thermal equilibration is about 4–5 min [37]. For the present short-transient-pulse technique, the relaxation time is 40 s at 12 K to be compared to 2–3 s for the heating time). If we suppose that the relaxation time in the 3.5 Hz ac method is at least ten times the periodic heating time, i.e. about 3 s, this value is much shorter than the relaxation time in the short-transient-pulse technique (about 40 s at 12 K). If we define the relaxation rate as $1/\tau$ and plot C_p/T^3 versus $1/\tau$, we obtain a similar tendency to that shown in the inset of figure 4.

Similar time-dependent effects are also observed for AsF_6. Figure 5 shows C_p/T^3 versus temperature for AsF_6, measured with different relaxation times: 'short' transient heat pulses, represented by ○ symbols in figure 5 (at $T = 4$ K, $\tau = 4$ s); and 'long' transient heat pulses, represented by ▲ symbols (at 4 K, $\tau = 13$ s). Very clearly, the specific heat depends on the relaxation time and on the period for which the heat has been applied. In order to increase this time of energy delivery, we have performed an additional experiment in the dilution cryostat with this time equal to 100 to 300 s. After the power was switched off, the relaxation was exponential (τ is typically 14 s at 4 K). We calculate the specific heat by integration of the relaxed energy through the thermal link. The data are shown in figure 5 (by □ symbols). One can see that a knee in C/T^3 at 3.5 K appears more clearly when the overall duration of the heat supply is increased.

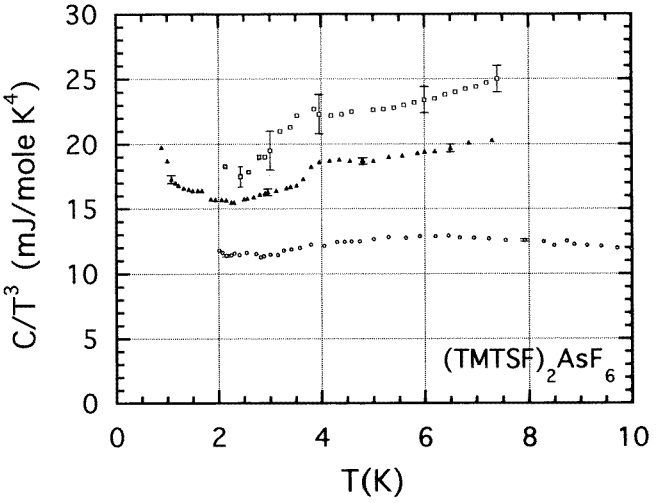

Figure 5. C_p/T^3 versus temperature for $(TMTSF)_2AsF_6$, measured with different transient techniques. ○ symbols represent the data derived by the 'short'-transient-heat-pulse technique ($\tau = 4$ s at $T = 4$ K) (this work). ▲ symbols represent the data derived by the 'long'-transient-heat-pulse technique ($\tau = 13$ s at 4 K), from reference [23]. □ symbols represent the data derived by the 'long'-transient-pulse technique, with heat delivery for 100–300 s ($\tau = 14$ s at 4 K), from reference [23].

As for PF_6 [22], we suggest that this knee measured at 3.5 K for AsF_6 is a manifestation of a glassy transition [23].

One might wonder whether there is some relation between the rate of cooling through the SDW transition and the large differences observed at low temperatures, as seen in figures 4 and 5. For our PF_6 experiments (figure 4), despite the cooling rate being estimated to be 4–5 times larger in the transient-heat-pulse experiment (□ symbols) than in the quasi-adiabatic one (▲ symbols), there is no difference between the data in the T-range from 3.5 to 7 K. Considering now AsF_6 (figure 5), the differences between the two upper data branches are clearly not related

to the cooling rate at T_{SDW}, since they were obtained during the same experimental low-T run below 8 K, without any reheating up to the transition. As a point of information, in figure 5 the data represented by ○ correspond to the usual cooling rate of ∼0.3 K h^{-1} at 12 K, whereas the data represented by ▲, □ correspond to a rate of ∼10 K h^{-1} at 12 K. We conclude that there is no such direct relation.

The time dependence of the specific heat is observed over the whole measurement temperature range, as its value is quite sensitive to the kinetics process, determined by t_H and τ, for PF_6, AsF_6 and Br compounds characterized by a SDW transition, while this phenomenon is *not observed* for the ClO_4 compound in the *metallic* state (with a superconducting transition at $T_c = 1.22$ K): C_p is then independent of the timescale of the experiment, measured either by 'long'- or 'short'-transient-heat-pulse methods [20] or by the ac ($f = 8$ Hz) method [39]. As an indicator of the experimental accuracy, we note the excellent agreement between the Debye temperature obtained by our transient method: $\theta_D = 216$ K [20] and that obtained by the ac method, for a sample composed of eight single crystals [39]: $\theta_D = 213 \pm 3$ K.

The origin of the time effects for salts with a SDW transition is still not understood. One suggestion is that they may be related to magnetic fluctuations in a large-T interval.

3.3. The SDW transition: estimation of the electronic contribution; electron–phonon coupling

Figure 6(a) shows the specific heat at the SDW transition for AsF_6 in a plot of C_p/T^3 versus temperature. The excess specific heat, dC_p, is determined by the subtraction from the total C_p of a background defined by a polynomial fit to the data (the solid curves in figure 6) slightly away from the transition (the data between 11.4 and 13.0 K being masked) in the same manner as is described in references [7, 40]. Such a method allows a good estimate of the excess dC_p to be obtained due to the relatively small temperature range ($\leqslant 1$ K) of the SDW transition. Figure 6(b) shows a similar analysis for PF_6 (carried out using data from this work).

3.3.1. The specific heat jump at T_c. The excess specific heats for PF_6, AsF_6 and Br plotted as dC_p/T versus temperature are shown in figure 7. The shape is perfectly symmetric, and is reminiscent of that for a first-order transition. However, we checked for first-order effects with great care by analysing the data for the transition region. We did not find any step in the perfect exponential decay of the sample temperature following the heat pulse, which means that no latent heat is involved during the transition within the experimental resolution. The peak position is very well reproducible when performing experiments with increasing or decreasing temperature (the cooling and heating rates are both 0.3 K h^{-1}). This means that no hysteresis was observed. Therefore, from our accurate measurements, we confirm that the SDW transition is a second-order transition without any first-order characteristics, like hysteresis and latent heat.

In figure 7(b), the solid curves represent a 'mean-field' (MF) analysis usually used for a second-order phase transition, which defines an ideal jump ΔC_p at the transition temperature T_c, by equalizing the entropy for experimental and idealized curves (the equal-area analysis: see reference [41]). From this figure, we can see that the SDW transition temperatures were found to be 12.2, 12.4 and 11.7 K for the PF_6, AsF_6 and Br compounds, respectively. The magnitudes of the normalized specific heat jump $\Delta C_p/T_c$ of the SDW transitions are 150.0, 88.0 and 19.0 mJ mol^{-1} K^{-2}, which means that the contributions for the SDW transition are 4.5%, 2.5% and less than 1% of the total specific heat for each sample, respectively.

Assuming that the jump is solely of electronic origin, we can estimate the electronic γ-coefficient in the metallic (or semiconducting) phase above T_{SDW}, using the usual mean-

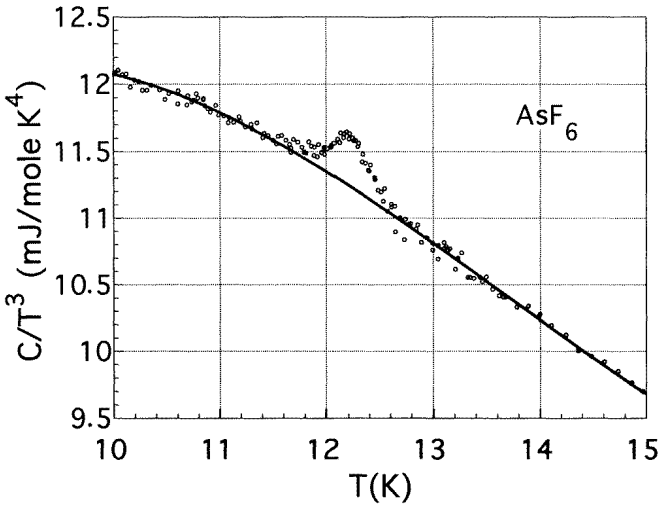

(a)

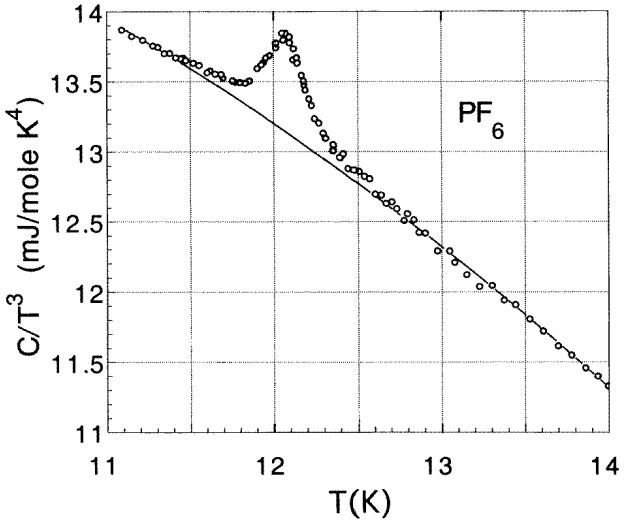

(b)

Figure 6. The SDW transition for (a) $(TMTSF)_2AsF_6$ in a plot of C_p/T^3 versus temperature and the polynomial background curve (solid curve) for obtaining the excess specific heat; and (b) $(TMTSF)_2PF_6$ (from this work, corresponding to the data represented by ○ in figure 4).

field BCS (Bardeen, Cooper and Schrieffer) expression $\Delta C_p/T_c = 1.4\gamma$ [42]. Although this analysis does not strictly satisfy entropy equality between the conducting (γ) state and the SDW semiconducting state [43], it enables a good estimation of the γ-value to be obtained from the jump. This gives $\gamma = 107.1$, 62.9 and 13.6 mJ mol^{-1} K^{-2} for PF_6, AsF_6 and Br, respectively. For PF_6, the γ-value is about one order of magnitude larger than that for metallic ClO_4, measured at low T [39]. When compared to previous measurements for PF_6, this value is found to be four times the γ estimated in reference [7] and about 20 times that estimated using the ac method reported in reference [9].

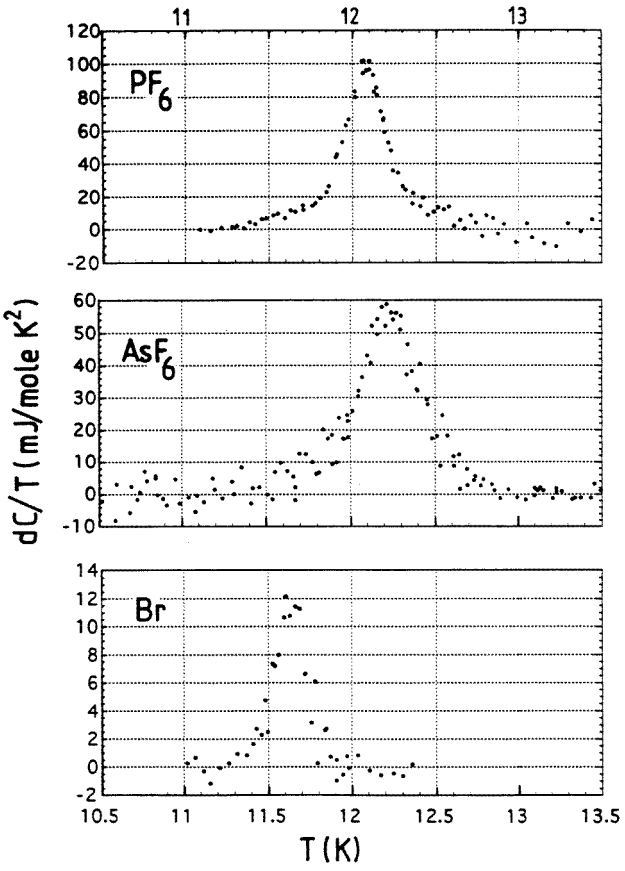

(a)

Figure 7. Excess specific heats for $(TMTSF)_2PF_6$, $(TMTSF)_2AsF_6$ and $(TMTTF)_2Br$, reported as dC/T. The solid curves in (b) represent a 'mean-field' equal-area analysis used to define the jump ΔC at T_c. Note that the data in (b) are the same as those in (a), but the scale has been changed to facilitate the analysis.

As regards these large discrepancies, two points are to be taken into account, which may be related:

(a) The inadequacy of the MF analysis to describe the transition. This was already pointed out for the CDW (charge-density-wave) transition of the blue bronze $K_{0.3}MoO_3$ [40, 44–46] and, to a lesser extent, for the SDW transition of PF_6 [9], with discrepancies for the values of γ estimated either from the entropy under the anomaly or the jump at T_c, which are always much larger than expected on the basis of other electronic properties. The discrepancy can reach an order of magnitude in the case of blue bronze [44]. A possible explanation is that phonon modes could be involved in the CDW transition, in view of the short coherence length, which also implies a large effect of critical fluctuations [47]. But such an explanation, based on a generic strong-electron–phonon-coupling character of the CDW transition, is probably inappropriate in the case of the SDW transition. Our present and previous [7] results show the substantial inadequacy of the MF interpretation for the SDW transition in PF_6, for which the electron–phonon-coupling character is currently a

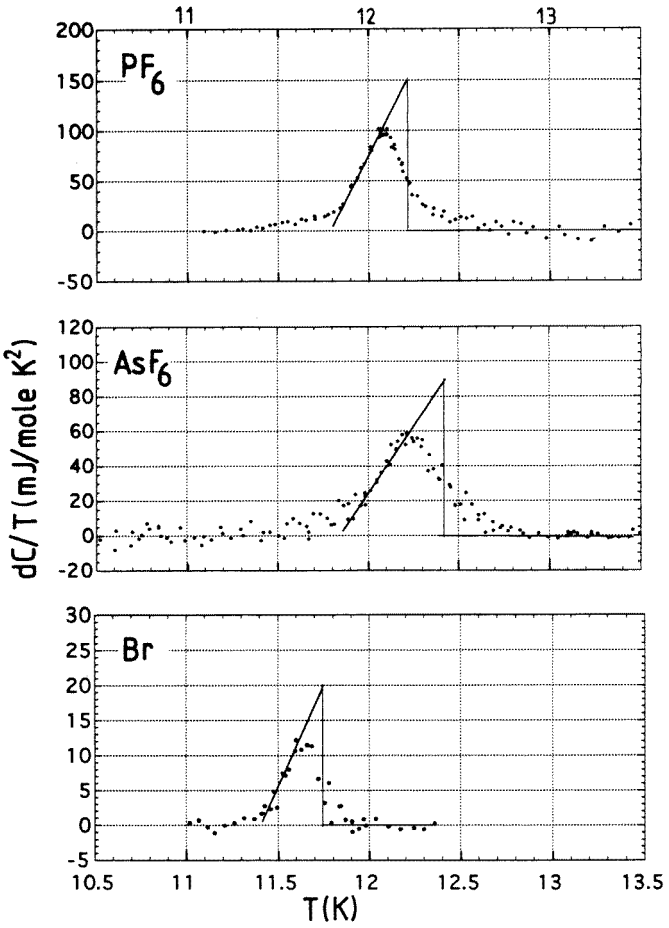

(b)

Figure 7. (Continued)

matter of debate. This point is discussed in the next subsection. An alternative explanation for the failure of the MF analysis could lie in fluctuation effects. In order to carry out a study of the critical behaviour, a very accurate determination of the lattice background is necessary, which is not possible in the present case due to the uncertainty of the electronic γ-term.

(b) Large variations in the magnitudes obtained for the jump by different authors and by different methods of C_p-measurement for the same compound. For instance for $K_{0.3}MoO_3$, Kwok and Brown obtain an excess specific heat of $\Delta C_p = 8$ J mol^{-1} K^{-1} [44] whereas Chung *et al* report ΔC_p ranging from 1.25 J mol^{-1} K^{-1} (reference [45]) to $\simeq$2 J mol^{-1} K^{-1} [46], depending on the background analysis.

3.3.2. Coupling to the lattice. One explanation proposed for the large discrepancy between the amplitude of the jump at T_c and the γ-value due to the electronic contribution is a possible coupling of the SDW to the lattice. In order to consider this problem in more detail, we have calculated the excess entropy $\Delta S = \int (\mathrm{d}C_p/T)\,\mathrm{d}T$ (with $\mathrm{d}C/T$ displayed in figure 7(a)). We

obtain the values 40.1, 30.9 and 2.9 mJ mol^{-1} K^{-1} for PF_6, AsF_6 and Br respectively. Using the temperature dependence of the gap very close to the transition, the change of the electronic energy was estimated in reference [9] to be $\Delta U_e = 0.2$ J mol^{-1} for PF_6. From our specific heat results, we obtain $T\,\Delta S = 0.49$ J mol^{-1}, which is about 2.5 times ΔU_e, although the estimate of ΔS is probably an underestimate since the extent of the anomaly is restricted to just ± 1 K away from T_{SDW}. In this case, we can suppose that ΔS has a component that is a lattice contribution. This suggestion is confirmed by recent x-ray measurements [16] where very weak satellite reflections were found below the SDW transition for PF_6. These results imply the possible existence of a CDW and so can explain the coupling of the SDW to the lattice.

4. Conclusions

We have measured the specific heats of the quasi-one-dimensional organic compounds $(TMTSF)_2X$ (X = PF_6, AsF_6 and ClO_4) and $(TMTTF)_2Br$ over the temperature range from 1.8 to 40 K.

The Debye-T^3 law is followed only at the lowest temperatures (below around 3 K) and C_p/T^3 exhibits a bump at about 7.0 K for each compound (4 K for ClO_4). The analysis of the experimental data shows that the phonon contribution shows a 3D behaviour below 3 K. Above this temperature the specific heat is described by a T^α-law ($\alpha = 2.4 \pm 0.1$) plus two additional Einstein modes of frequency 30–35 K and 65 K, which are in good agreement with the low-frequency modes at 18 cm^{-1} and 40 cm^{-1} observed in far-IR spectroscopy for $(TMTSF)_2PF_6$. These results indicate the large anisotropy of the force constants along and between adjacent chains and the contribution of low-lying optical modes inherent to the structural properties of one-dimensional systems.

The glasslike transition at 3.5 K in the case of $(TMTSF)_2PF_6$ (and $(TMTSF)_2AsF_6$) involves a part of the C_p/T^3 bump originating from configurational excitations; but up to now we have no more precise argument for a possible relation between the low-frequency phonon modes and the occurrence of this type of transition.

The spin-density-wave (SDW) transition temperatures were found to be 12.2, 12.4 and 11.7 K for the $(TMTSF)_2PF_6$, $(TMTSF)_2AsF_6$ and $(TMTTF)_2Br$ compounds, respectively. The present measurements confirm that the magnitude of the specific heat anomaly for $(TMTSF)_2PF_6$ (4.5% of the total specific heat at the transition temperature) is too large to be explained by the electron spin contribution alone, which implies that the lattice is also involved in the transition. From our accurate measurements, we confirm that the SDW transition is a second-order transition without any first-order characteristics, like hysteresis and latent heat.

The specific heat is found to be time dependent over the whole measurement temperature range, as its value is quite sensitive to the kinetics process for all three compounds. A more detailed analysis of the frequency dependence of the specific heat is clearly needed.

Acknowledgments

Samples were kindly provided by K Bechgaard ($(TMTSF)_2PF_6$, Denmark), H Anzai ($(TMTSF)_2AsF_6$, Japan), J M Fabre ($(TMTTF)_2Br$, Montpellier) and C Lenoir and P Batail ($(TMTSF)_2ClO_4$, Orsay). We would like to thank D Staresinić and K Biljaković for their contribution to the measurements of $(TMTSF)_2AsF_6$ by another technique and for stimulating discussions.

References

[1] For a review, see
Jérome D and Schulz H J 1982 *Adv. Phys.* **31** 299
Saito G and Kagoshima S (ed) 1990 *The Physics and Chemistry of Organic Superconductors (Springer Proceedings in Physics vol 51)* (Berlin: Springer)
Monceau P and Brazovskii S (ed) 1993 *Proc. ECRYS-93: Int. Workshop on Electronic Crystals (Carry le Rouet, 1993); J. Physique Coll.* IV C2 **3**
Farges J P and Dekker M (ed) 1994 *Organic Conductors* (New York)
[2] Jérome D 1994 *Solid State Commun.* **92** 89
[3] Chaikin P M, Choi M Y, Kwak J F, Brooks J G, Martin K P, Naughton M J, Engler E M and Greene R L 1983 *Phys. Rev. Lett.* **51** 2333
Ribault M, Jérome D, Tuchendler J, Weyl C and Bechgaard K 1983 *J. Physique Lett.* **44** L953
[4] Danner G, Kang W and Chaikin P M 1994 *Phys. Status Solidi* b **201** 442
Danner G, Chaikin P M, Kang W, McKernan S and Hannahs S T 1995 *Synth. Met.* **70** 731
[5] Nomura K, Hosokawa Y, Matsunaga N, Nagasawa M, Sambongi T and Anzai H 1995 *Synth Met.* **70** 1295
[6] Lasjaunias J C, Biljaković K, Monceau P and Bechgaard K 1992 *Solid State Commun.* **84** 297
[7] Odin J, Lasjaunias J C, Biljaković K, Monceau P and Bechgaard K 1994 *Solid State Commun.* **91** 523
[8] Lasjaunias J C, Biljaković K and Monceau P 1996 *Phys. Rev.* B **53** 7699
[9] Coroneus J, Alavi B and Brown S E 1993 *Phys. Rev. Lett.* **70** 2332
[10] Le L P *et al* 1993 *Phys. Rev.* B **48** 7284
[11] Takahashi T, Maniwa Y, Kawamura H and Saito G 1986 *J. Phys. Soc. Japan* **55** 1364
[12] Delrieu J M, Roger M, Toffano Z, Moradpur A and Bechgaard K 1986 *J. Physique* **47** 839
[13] Barthel E, Quirion G, Wzietek P, Jérome D, Christensen J B, Jorgensen M and Bechgaard K 1993 *Europhys. Lett.* **21** 87
[14] Nakamura T, Nobutoki T, Kobayashi Y, Takahashi T and Saito G 1995 *Synth. Met.* **70** 1293
[15] Requardt H, Currat R, Monceau P, Lorenzo J E, Dianoux A J, Lasjaunias J C and Marcus J 1997 *J. Phys.: Condens. Matter* **9** 8639
[16] Pouget J P and Ravy S 1996 *J. Physique* **6** 1501
Pouget J P and Ravy S 1997 *Synth. Met.* **85** 1523
[17] Bechgaard K, Carneiro K, Rasmussen F, Olsen M, Rindorff G, Jacobsen C S, Pedersen H J and Scott J C 1981 *J. Am. Chem. Soc.* **103** 1440
[18] Delhaes P, Coulon C, Amiell J, Flandrois S, Torreilles E, Fabre J M and Giral L 1979 *Mol. Cryst. Liq. Cryst.* **50** 43
[19] Lasjaunias J C and Monceau P 1982 *Solid State Commun.* **41** 911
[20] Yang Hongshun, Lasjaunias J C and Monceau P 1999 to be published
[21] Wun M and Phillips N E 1975 *Cryogenics* **15** 36
[22] Lasjaunias J C, Biljaković K, Nad' F, Monceau P and Bechgaard K 1994 *Phys. Rev. Lett.* **72** 1283
[23] Lasjaunias J C, Biljaković K, Starešinić D, Monceau P, Takasaki S, Yamada J, Nakatsuji S and Anzai H 1999 *Euro. Phys. J.* B **7** 541
[24] Lasjaunias J C, Monceau P, Starešinić D, Biljaković K and Fabre J M 1997 *J. Physique* I **7** 1417
[25] See, e.g.,
Gopal E S R 1966 *Specific Heats at Low Temperatures* (New York: Plenum) ch 2, p 31
[26] Konaté K 1984 *PhD Thesis* Université de Grenoble
[27] Odin J, Hasselbach K, Biljaković K, Lasjaunias J C and Monceau P 1999 to be published
[28] Odin J, Lasjaunias J C, Berton A, Monceau P and Biljaković K 1992 *Phys. Rev.* B **46** 1326
[29] Biljaković K, Lasjaunias J C, Zougmoré F, Monceau P, Levy F, Bernard L and Currat R 1986 *Phys. Rev. Lett.* **57** 1907
[30] Eldridge J E and Bates G S 1985 *Mol. Cryst. Liq. Cryst.* **119** 183
[31] (a) Ng H K, Timusk T and Bechgaard K 1983 *J. Physique Coll.* **44** C3 867
(b) Challener W A, Richards P L and Greene R L 1983 *J. Physique Coll.* **44** C3 873
[32] Harper J M E, Greene R L, Grant P M and Street G B 1977 *Phys. Rev.* B **15** 539
[33] Wunderlich B and Baur H 1970 *Adv. Polym. Sci.* **7** 151
[34] Reese W 1969 *J. Macromol. Sci. Chem.* **3** 1257
[35] Biljaković K, Lasjaunias J C and Monceau P 1991 *Phys. Rev.* B **43** 3117
[36] Genensky S M and Newell G F 1957 *J. Chem. Phys.* **26** 486
[37] Lasjaunias J C, Odin J, Biljaković K, Monceau P and Bechgaard K 1993 *J. Physique Coll.* IV **3** C2 365
[38] Biljaković K, Lasjaunias J C, Monceau P and Levy F 1989 *Europhys. Lett.* **8** 771

[39] Garoche P, Brusetti R, Jérome D and Bechgaard K 1982 *J. Physique Lett.* **43** L147
Brusetti R, Garoche P and Bechgaard K 1983 *J. Phys. C: Solid State Phys.* **16** 3535
[40] Kwok R S, Gruner G and Brown S E 1990 *Phys. Rev. Lett.* **65** 365
[41] Zougmoré F, Lasjaunias J C and Béthoux O 1989 *J. Physique* **50** 1241
[42] See, e.g.,
Ashcroft N W and Mermin N D 1981 *Solid State Physics* (New York: Holt-Saunders) ch 34, p 745
[43] In an exact MF analysis, one has to take into account the γT-contribution for $T \leqslant T_c$, in addition to the lattice term used as the 'background'. Due to the smallness of the experimental jump of C_p at T_c (less than 3% of the total C_p for PF_6), and the absence of any discontinuity in C/T^3 below T_c (see for instance figure 6(a)), we have approximated the 'background' lattice from the experimental data, i.e. ignoring the electronic contribution below T_c.
[44] Kwok R S and Brown S E 1989 *Phys. Rev. Lett.* **63** 895
[45] Chung M, Kuo Y K, Mozurkewich G, Figueroa E, Teweldemedhin Z, DiCarlo D A, Greenblatt M and Brill J W 1993 *J. Physique Coll.* IV **3** C2 247
[46] Brill J W, Chung M, Kuo Y K, Zhan X, Figueroa E and Mozurkewich G 1995 *Phys. Rev. Lett.* **74** 1182
[47] McMillan W L 1977 *Phys. Rev.* B **16** 643